Hindawi
Mathematical Problems in Engineering
Volume 2022, Article ID 4911952, 10 pages
https://doi.org/10.1155/2022/4911952

Research Article

An Index for Rail Weld Health Assessment in Urban Metro Using In-Service Train

Morad Shadfar, Habibollah Molatefi, and Asghar Nasr

Iran University of Science and Technology, Tehran, Iran

Correspondence should be addressed to Habibollah Molatefi; molatefi@iust.ac.ir

Received 8 October 2022; Revised 27 November 2022; Accepted 30 November 2022; Published 27 December 2022

Academic Editor: Madalina Dumitriu

Rail welds are considered as the weak part of a railway track. Their defects and health can directly affect wheel-rail interaction, track safety, and reliability. Current practices for rail welds health assessment are based on 2D vertical and lateral wear measurement which needs time and track blocking. The development of inertia-based condition monitoring methods such as measuring axle box acceleration (ABA) comes with a crucial question on criteria or index for each rail track component health monitoring. In this study, an index for evaluation of rail weld health is proposed through integrated numerical and field experiment data within a metro line using the ABA technique. The relationship between the speed, wheel structural vibration, and acceleration amplitude is investigated using fast Fourier transformation (FFT) and a nonlinear neural network principal component analysis (PCA) model. An index is introduced to assess weld severity level based on the statistical method. This index is simple and applicable for maintenance practice.

1. Introduction

Rail track maintenance actions are divided into three categories according to EN13848-5 standard: alert limit (AL), intervention limit (IL), and immediate action limit (IAL) [1]. The basis for identifying defects and determining the priority of each repair is done using track recording vehicles (TRVs) which implement data collection at intervals of about 0.25 m. Therefore, defects with very short wavelengths (such as worn weld, rail spalling, and corrugation) cannot be detected in this way. Most railway operators use visual inspection and nondestructive testing (NDT) methods to identify local defects. The main challenge in visual inspection is the possibility of human error and inaccurate estimation of the severity of defects. Also, the use of NDT requires track occupation which limits the use of these methods for high-traffic corridors. Current standards for rail welds inspection are based on measuring vertical and lateral wear which do not consider welds geometry, wheel-rail interaction, and contact forces which is an indication of track deterioration.

Using in-service train acceleration for maintenance purposes is introduced to cover the abovementioned challenges. The accelerometer is mounted on the axle box and by analyzing the collected acceleration data, information can be obtained about the rail defects. Extensive work has been done by Molodova et al. in this area [2–6]. They were able to identify squat defects in a railway track through wavelet analysis. It is also possible to determine the bolts preload in fishplates using this method [7]. Núñez et al. in 2018 used the ABA technique to establish a cost-effective inspection and asset management to minimize maintenance intervention time/cost without dedicated inspection vehicles [8]. In 2018, Bocz et al. with the help of the ABA and scaled average wavelet power (SAWP) studied possibility of the tramway track condition monitoring [9]. In 2021, Cho and Park used the ABA to detect squats in the Korean railway using wavelet spectrum. They concluded that the most probable areas for squats formation are rail welds and joint sections [10]. In 2022, Xu et al. with the help of the ABA method estimated rail corrugation in a high-speed track using the energy factor and inverse STFT method [11]. The use of axle box acceleration for condition monitoring of a track has been taken into consideration by many railway's companies in recent years. This method is based on the

instantaneous response of the wheel when passing through a defect [3]. So, if the track deteriorates, accelerations are modified and through studying their changes in frequency contents, defects can be monitored.

Similar to track geometry, evaluation of rail weld wear is implemented using versine (1 m for rail weld), which only considers longitudinal rail surface irregularity where geometry, contact forces, velocity and other possible parameters are not considered [12]. Also, there is a research gap where there is a demand for the introduction of an index available using contact force to determine track health. The input parameters for this purpose are speed, location, and vertical acceleration. In the next step, an index is developed for defect identification with the help of short-time Fourier transformation (STFT), wheel structural natural frequencies, and nonlinear neural network PCA. The data obtained from the field test were analyzed and practical examples of the application of this method are presented. The presented index can be used for practical applications in track maintenance operations.

2. Rail Track

The structure of a railway track consists of two rails fastened to the sleepers. The force transmission path is from the wheel to the rail and then the fastening system, sleepers, and superstructure. At constant intervals, the rails are welded together, which are usually the weak points that are susceptible to failure. Rail defects can be classified into 3 distinct categories (from a wheel point of view): rail welds, rail defects in the area between the two sleepers, and track defects in the sleeper area.

In a rail system, the real challenge of using the ABA method is to examine acceleration changes over time. Unlike a closed system, the railway track is very long and also the corridor can have two or more tracks. In practice, identifying the position and severity of the impact provides sufficient information for maintenance personnel. For this purpose, a simple odometry algorithm based on complementary analysis of signaling system data can be used for defect positioning. Odometry can be defined as the use of data from motion sensors to estimate changes in position over time [13]. Various methods and techniques have been proposed to increase the accuracy of signaling systems, including the use of trackside equipment, sensor fusion, and a combination of existing methods. In 1996, Mirabadi et al. reviewed different train positioning methods and examined the possibility of increasing positioning accuracy using sensor fusion [14]. In 2002, Allotta et al. developed an algorithm using neural network, fuzzy logic, and crisp logic which can estimate train speed with the help of wheel speed data. Their proposed algorithm can keep its accuracy even for poor wheel and rail contact conditions [15]. Also, in 2011, they examined different scenarios for their speed estimation algorithms in different conditions such as failure of one or more sensors and acceleration/braking process and compared their algorithm error with the existing signaling system [16]. In 2013, with the help of a tachometer, inertia sensors, and sensor fusion, they modified the accuracy of the existing odometry algorithm in the Italian railway signaling system. Their work's importance was in overestimating the available braking distance for the train, which endangers safety. Based on Kalman's filter theory, a sensor fusion was performed on tachometer and gyroscope data to eliminate noise effects. Results showed a significant improvement in the accuracy of train speed estimation [17].

The odometry algorithm used to detect welds is shown in Figure 1; the reference is rail welds. The input data are speed and position data that are read from various sources (signaling system, GPS, tachometer, etc.) and axle box acceleration (vertical) for left and right wheels. The acceleration data are then analyzed to detect weld impacts. Weld detection criteria can also vary from a simple maximum to linear regression and complex signal processing techniques and pattern recognition depending on the nature and quality of the signal. After detecting rail welds, their position can be modified. The acceleration data for left and right rails with different inputs can also compete with each other to achieve the highest accuracy.

It is worth noting that all the odometry algorithms need a reference to map the data in order to track any desired parameters. In this case, the first measurement is considered as reference and all recordings are mapped relative to that.

Therefore, a modified displacement is obtained, in which the values of vertical acceleration are analyzed relative to that. So, in repeated data acquisition, the signal points are mapped to each other for monitoring purposes. At this stage, the position of all points in terms of sleeper, welds and the area between the two sleepers can be easily calculated. Figure 2 shows the output of the algorithm for detected rail welds. It can be seen that for both types of tracks (straight and curved), the algorithm has successfully identified the position of the welds.

These impacts have been influenced by many parameters, including speed and weld severity. So, an index is required to access the impact nature and action level.

3. Weld Defect Detection Method

This section provides a criterion for detecting rail weld defects with the help of field test data. As track components deteriorate, their dynamic interaction responses will alter accelerations on the train. So, studying these changes would help us to detect defect states. So, axle box acceleration data are measured in a metro track and its relation with speed, structural vibration of wheels, and other parameters are needed to be considered.

In order to minimize the effects of train dynamics on wheel-rail interaction, the leading axle is used for data acquisition; therefore, the influence of track parameters, including the associated natural frequency and stiffness (like bridges, ballasted, or slab tracks) and gearbox vibrations can be detected, and they are already considered through this method (it is discussed in detail in reference [18]). The presented method is able to detect all impacts including rail weld and other types of rail surface defects. Also, corrugation can be detected as it is explained in reference [18]; the focus of this study is to detect rail welds to present the proposed method.

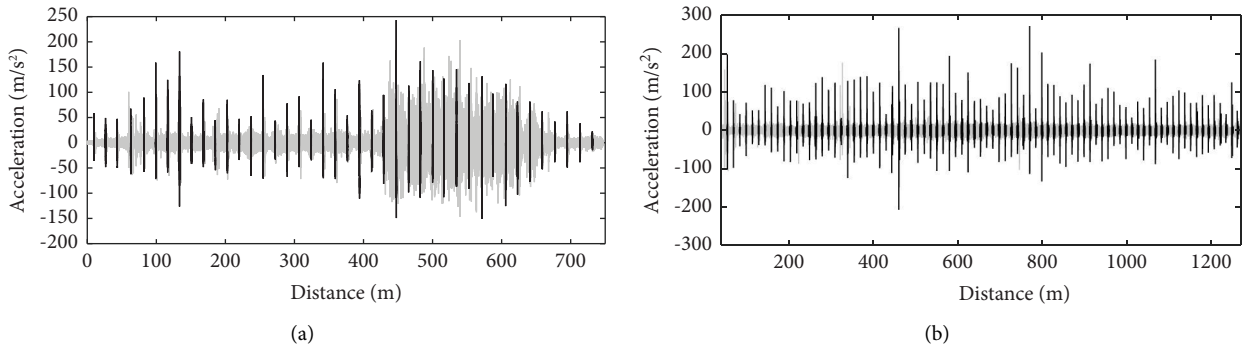

Figure 1: Welds impacts in a metro track for a) curved track and b) straight track.

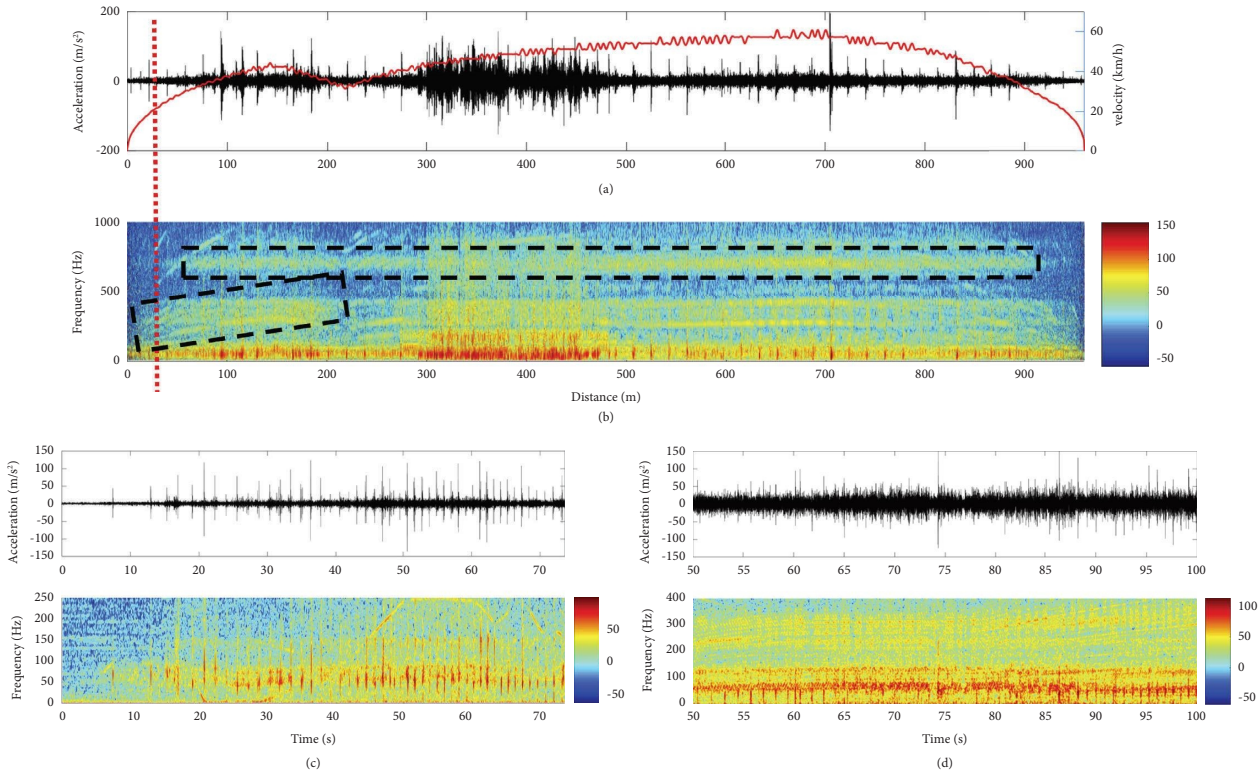

Figure 2: An example of measured axle box acceleration in a) line 1 and time domain and b) line 1 and calculated STFT in dB c) line 3 and d) line 5 for an electric locomotive.

First, the weld impacts are found based on the odometry explained in Section 2; a nonlinear PCA method presented by Scholz [19] is used to study the relationship between impact severity and speed. Based on the results obtained in this part, the accelerations are weighted by their speed. This PCA method uses a neural network. Two approaches can be considered: circular, which fits the data into a circle and inverse, which fits a curve into the data. For this study, since the nonlinear relation between impacts and their speed is required, the inverse method is used.

Figure 3(a) shows an example of vertical acceleration and its calculated short-time Fourier transformation (STFT). This test is conducted online 1 of Tehran metro with an Aluminum 500 series metro car. Figure 3(c) shows results for a carbon-steel train in Line 3 and Figure 3(d) shows measured data from an electrical locomotive in Line 5 of Tehran urban metro, which is different in train and track characteristics. Based on reference [20], a window size of 0.125 s points would result studying any parametric excitation which is used in this study. This signal contains tangent and curved sections (distance 300–500 m). For better illustration, the STFT results are plotted in dB.

Vertical axle box accelerations contain both velocity-dependent and velocity-independent components. The velocity-dependent vibrations are basically due to gearbox vibration (which is shown in Figure 3(b)). They follow the velocity profile pattern. So, a change in speed would change this frequency. Weld impacts are also change with changes in train speed, which will be discussed later.

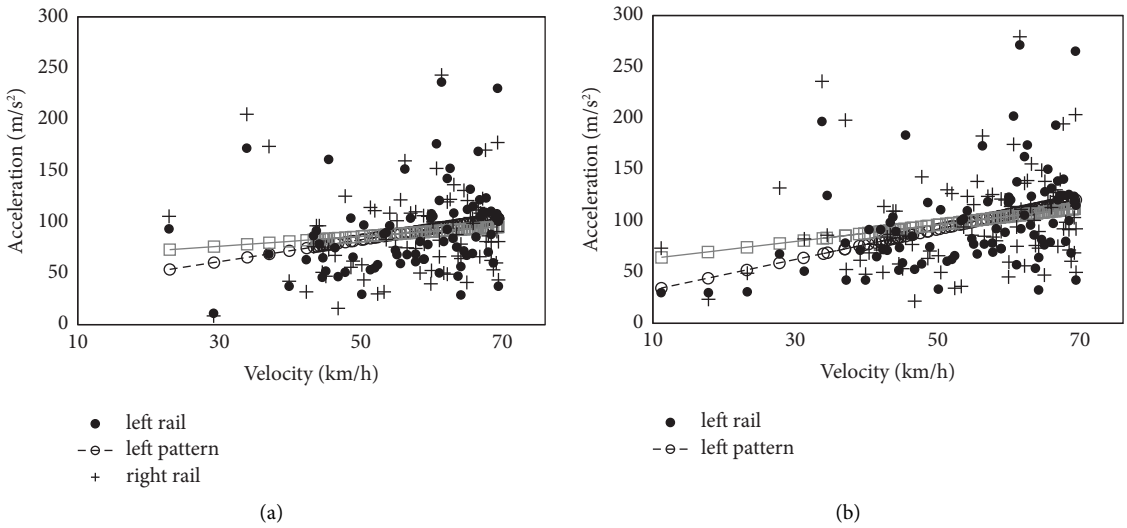

Figure 3: Weld impacts variation with speed and their relation.

Velocity-independent type is referred to as wheelset structural mode shapes. An example of such a component is shown in Figure 3(b). These modes' amplitude can change with speed or excitation type, but the frequency is constant. The recorded wheelset mode shapes frequencies in the test are 73, 86, 136, 285, 355, 449, and 679 Hz. The weld has excited wheel mode shapes up to 680 Hz. These modes affect the measured signal and their amplitude can be used for judging impact severity. For each impact, wheel mode shapes are excited. The more the impact energy, the higher modes amplitude are expected. This is verified through all test data for about 27 km track of line 1, line 3 and 5 and repeated data acquisition. More details can be found in reference [18].

A critical point about using the ABA method is that the wheel profile needs to be in good condition. So, the track components would become dominant in the recorded data. For all test presented in this research, the train was at a good condition and wheel profile was almost new. In case of any wheel damage, it follows a frequency proportional to velocity which can be distinguished and removed.

In order to find a good index to evaluate weld impacts and obtained results, the following parameters are considered:

(i) Vertical acceleration: Raw data used for calculating wheel vibration modes and impact force

(ii) Wheel vibration modes: The sum of the mode shapes amplitude are used for defect detection [21, 22]

(iii) Speed: it has a linear effect on increasing the impact intensity [12].

The results are analyzed and three different approaches are examined: weighted accelerations, wheel mode amplitude summation (WMAS) to clear out components unrelated to the impact, and weighted WMAS to consider accelerations at low speed.

After identifying the rail welds in the measured signal, it is necessary to study the severity of the failure and prioritize them. The measured points can be treated as statistical data. The railway tracks between two stations are built with similar materials, almost the same life span and were built with the same quality. So, it can be assumed that the data points should behave similarly. Therefore, the differences in some of the data points can be considered as a preliminary guess about the probability of a failure. The detected weld impacts in Figure 2 are plotted in terms of the corresponding velocity in Figure 4. These welds are built at the same time and with the same quality. Therefore, it is expected that the amplitudes will be closer to each other by eliminating the effect of speed. Using the nonlinear PCA method, the relationship between velocity and impact amplitude is found to be linear. This linear pattern is also reported and confirmed by Esveld and Steenbergen [12].

According to the obtained result, the results can be weighted with speed. So, the impacts from different speed can be compared with each other. Figure 5 shows the results of the acceleration amplitude of the weld and weighted accelerations by velocity. By dividing the acceleration to velocity at very low speed, the results tends to infinity. Also, this method is based on vibration mode amplitude. So, the assumption of structural vibration of wheelset shall be fulfilled. To cover this challenge, a threshold (limit velocity) must be considered for the weighted values. Thus, at speeds above the limit value, the sum of the amplitudes of the modes is divided by the speed, and at speeds below it, it is divided by a limit value or replaced by zero. This limit value can be determined by which wheel mode shapes amplitude (Figure 4(b)) starts to be nonzero. It is assumed that when all considered wheel mode shapes start to vibrate, the axle box vibration can be analyzed as dynamic. In this study, this threshold is calculated as 20 km/h and is shown as vertical dashed line in Figures 4(a) and 4(b). Change in this limit velocity has a minor effect in the final results and depends on the contractor policy. Because in small portion of the track, the train has a velocity below the limit value.

In the next step, statistical distribution for weld impacts is studied. The velocity-weighted data are found to follow the

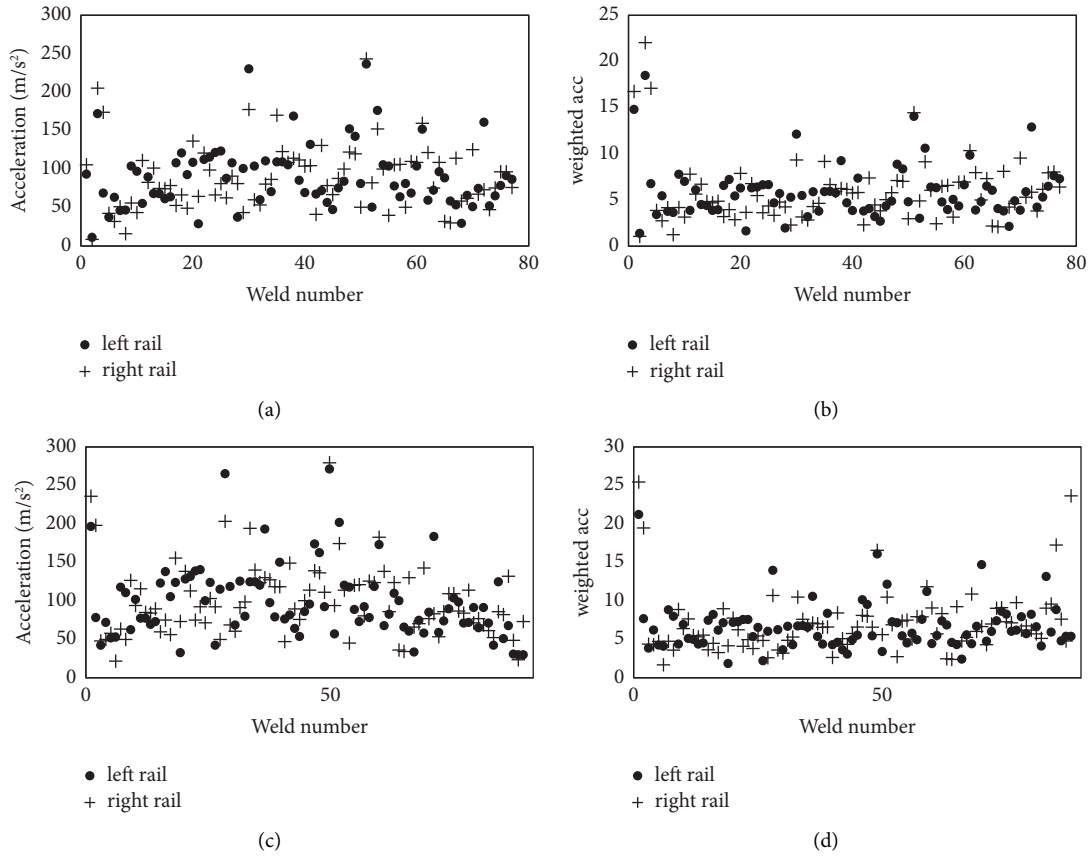

Figure 4: Weld impacts (up) and their weighted values (down) for a curved (left) and straight (right) track.

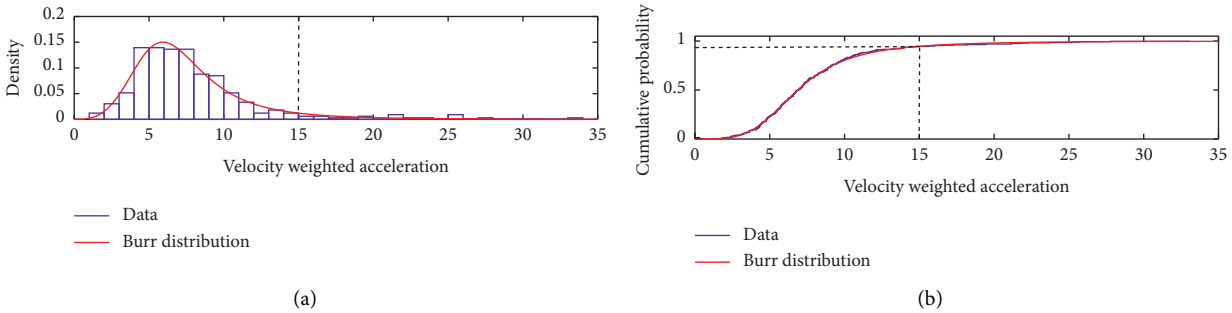

Figure 5: Distribution of weld data.

Burr distribution, as is shown in Figure 6. This distribution is perfect for a nonnegative random variable. The confidence level is 95% and both density and cumulative probability show good fitting with the data. The dashed line represents impacts that are lower than the upper bound of the 95% reliability interval. So, the upper 5% can be scheduled for inspection and maintenance. The probability density function and cumulative distribution function are defined as follows:

$$f(x;c.k) = ck\frac{x^{c-1}}{\left(1+x^{c}\right)^{k+1}},$$
$$f(x;c.k) = 1-\left(1+x^{c}\right)^{-k}. \quad (1)$$

In addition to velocity-weighted impacts along with the impact factor, another approach can be considered. The acceleration signal contains components unrelated to the impact, such as gearbox vibration or rail roughness. However, the wheel mode shapes are excited directly at the instance of the impact and can be used as an indicator to assess the impact intensity, more accurately. The frequencies of wheel modes are constant but their amplitude has a linear relationship with velocity. The more severe the impact, the more modes are excited. In practice, the first four modes of the wheel (up to 355 Hz) are affected by the impact, but for large impacts, up to the first six modes (up to a frequency of 700 Hz) should be considered [22].

Results for wheel mode shapes amplitude summation for the first six wheelset mode shapes are shown in Figure 7. The

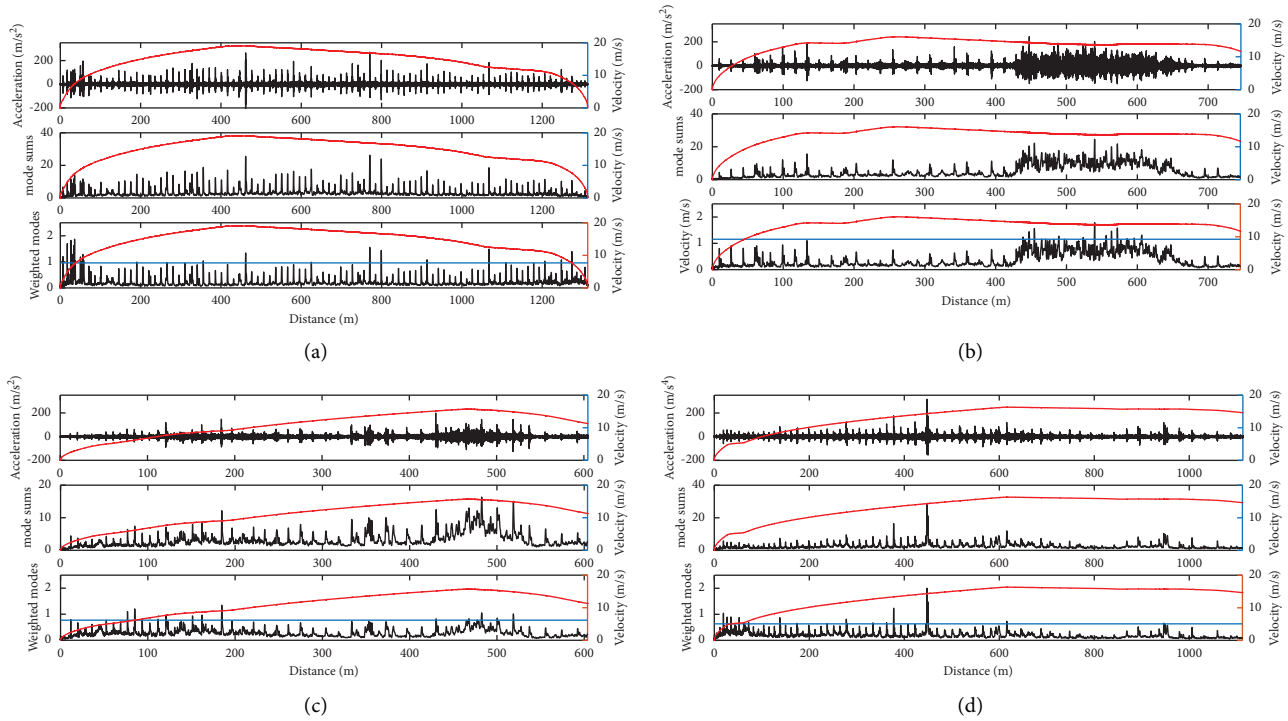

Figure 6: WMAS and velocity-weighted WMAS. a) test code: ABA_SN_346_0506, b) test code: ABA_SN_346_1314, c) test code: ABA_SN_346_1718, and d) test code: ABA_SN_346_2526.

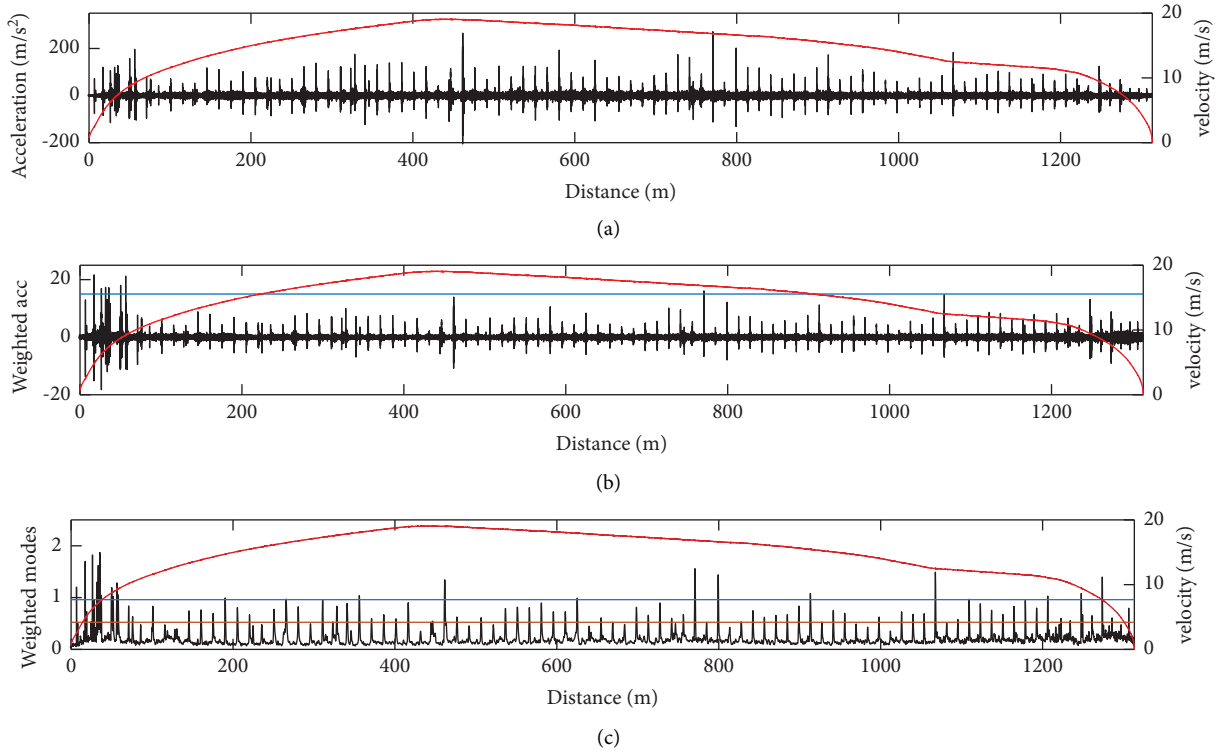

Figure 7: Comparison of two method output (test code: ABA_SN_346_0506).

vertical acceleration signal, the sum of six amplitudes of the wheel vibration modes (neighborhood of 20 Hz for each mode), and the weighted mode sum are plotted in each figure. The impacts are compared relative to each other. So, the basic logic, in this case, is that a point that is different from the others should be inspected. Such difference of weld

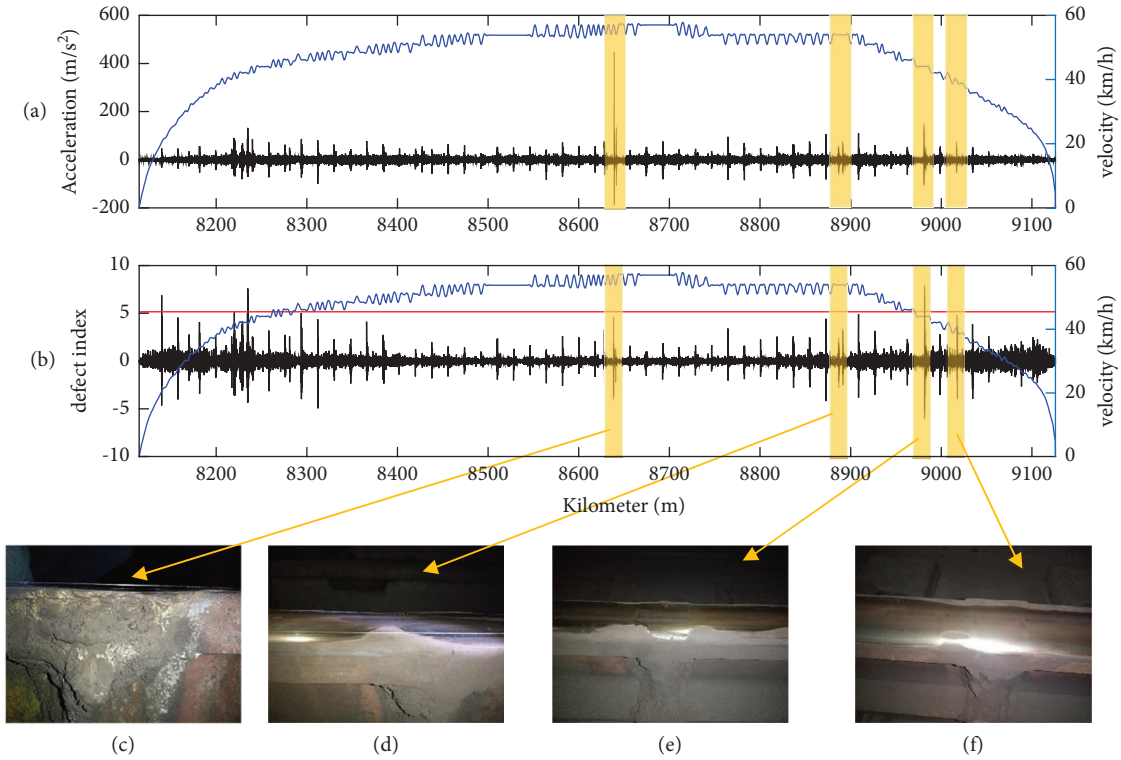

Figure 8: Measured acceleration (a) and inspected defects using weighted acceleration (b).

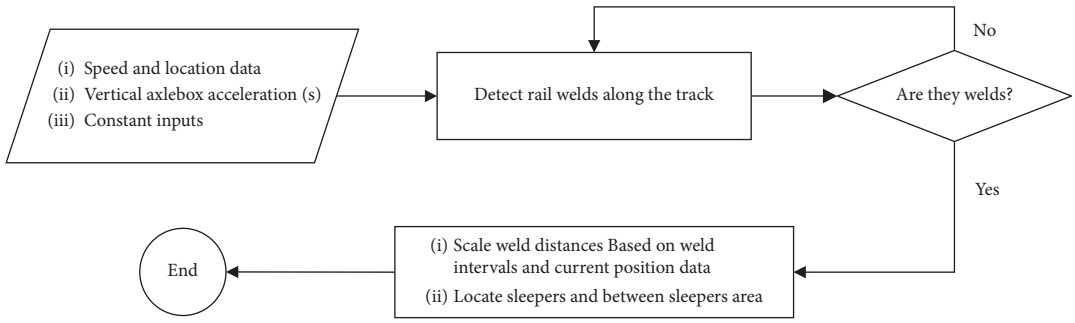

Figure 9: Train positioning algorithm.

with the others, its type and values, indicates the necessity of this criterion in this section. Also, the points can be compared generally or locally. All the welds in a corridor can be compared with each other or only welds in a specific area, for example, the distance between two stations. This assumption can be applied to all methods presented in this study and will be discussed later.

In the results, any point which shows a higher impact eventually has a peak. Considering the linear relationship between acceleration amplitude and velocity, values are weighted with velocity. This weighting is a more appropriate criterion for decision making about weld defects. In order to ensure that the large acceleration at low speed is not ignored, the velocity-weighted WMAS method is used for subsequent analysis. Figure 7 shows a comparison of the WMAS and velocity-weighted WMAS values. The velocity profile is also displayed and the horizontal line in the weighted values indicates that 99% of the data are below this line. This line is a good criterion for labeling the severity of the impact and it can be said that the points (areas) above this line should be inspected. The 99% limit can vary for different rail networks depending on the reliability of welds or network, safety, workforce, and workload available. So, it can be formulated as follows:

Table 1: Sources for errors and measures to cover it.

Action in procedure	Potential and occurred error	Effect on results	Root cause	Taken action
Sensor arrangement	(i) Improper accelerometer	High	Unable to record desired pattern and frequencies	(i) A preliminary test is one to determine proper accelerometer capacity.
	(ii) Low accuracy of arrangement	Medium	Effects of vehicle dynamic on results	(i) Other references are checked for an optimum arrangement. (ii) The leading wheel is used to minimize vehicle effect.
Data acquisition	(i) Unwanted noise	Medium	Electromagnetic and mechanical vibration	(i) Static test is done to determine background noise. (ii) Shielded cables are used.
	(ii) Vehicle vibration	Medium	Vehicle dynamics	(i) Vehicle dynamics effects are determined as velocity-dependant vibration and cleared from the results if needed.
Data processing	(i) High computational volume	Low	(i) High volume of measured data (ii) Modern methods required higher computation time	(i) Optimum parameters for windowing, method, etc., are chosen to minimize calculation time.
Pattern extraction and index definition	(i) Vehicle location error (ii) Change in velocity (iii) Repeatability (iv) Comprehensiveness of results	Medium	(i) Odometry and signalling error (ii) Normal operation of the train (iii) Possible fake impacts in results (iv) Change in train and track characteristics	(i) An innovative odometry algorithm is developed to control fault location error based on rail welds locations. (ii) Normalizing the acceleration with velocity and setting a limit velocity for low speed. (iii) Repeated data acquisition on different tracks with different train and track characteristics is made to check the repeatability and comprehensiveness of the presented algorithm.

$$\text{impact index} = \left(\frac{\sum_{i=1}^{6} \text{mode amplitude}_i}{v} \right)_{\%99} \quad v = \begin{cases} V_{\text{limit}}, & \text{velocity} < V_{\text{limit}}, \\ \text{velocity}, & \text{velocity} > V_{\text{limit}}, \end{cases} \tag{2}$$

The limit value, as it is mentioned above, is 20 km/h. Calculated WMAS and weighted WMAS values below this limit velocity will have lower amplitude magnification which is still high enough for inspection alarm as it is indicated in Figure 7.

The interesting point in Figure 7 is the impacts at low speeds almost at the beginning of the signal. For example, in Figures 7(a) and 7(d), large accelerations (considering the speed) are spotted despite the low speed. For example, there are some cases where the train must accelerate on a sharp curve to start moving, which is difficult to identify without weighing the components relative to speed.

A comparison of the two proposed methods including weighted acceleration and velocity-weighted WMAS is shown in Figure 8. Figure 8 represents the difference in nature between comparing weld data generally and locally. Figure 8(b) shows the weighted acceleration along the 95% line and Figure 8(c) shows the sum of the modes along with the 99% and 98% lines. It can be seen that the weighted acceleration resulted in fewer inspection points. The reason for this is the difference in assumptions between these two methods. Weighted acceleration compares all the welds in a network or corridor, while the velocity-weighted WMAS compares the welds in a small area (distance between two stations in this case). The assumption of comparison of the points generally or locally can be applied to either of these two methods, and the number of inspection points (as it is mentioned) is a function of the operation parameters and safety.

4. Checking the Results

To evaluate the accuracy of the results, the test is repeated with a sampling frequency of 10 kHz. An accelerometer's natural frequency is 2500 Hz. The data are analyzed using the weighted acceleration method presented in this study. An example of the measured data along with the velocity-weighted one is presented in Figure 9.

Four cases are examined. Photos taken from faulty detected rail welds are also shown. Between the distances 8200 and 8300, there is a switch. In case 1, there is a 3 mm vertical step due to wear which lead to a high impact in raw data but weaken because of velocity. Still, it is close to the criteria line. For cases 2 and 4, a minor wear at the end of rail weld is observed and is shown in Figures 9(d) and 9(f). Case 3 is a serious major deterioration in rail weld and as it can be seen in Figure 9(e), high local wear has occurred at weld ends which will result in high impacts and eventually rail break.

Another point emphasizing this method's advantage is that all of these cases were missed by maintenance personnel (especially case 1 and 3 which are rejected welds) due to the improper light condition inside of the tunnel.

The presented algorithm, the weld with index greater than the defined threshold (1 or 2% which is explained), is considered as defective weld. However, leaving the judgment to the machine instead of human expert needs large data gathering and database. The algorithm as it is now is a tool to help the personnel to priorities their schedule and after gathering a proper dataset the condition monitoring system can be established.

In order to examine possible error sources and their effects on results accuracy, each potential and occurred noise and error are presented in Table 1 and actions to cover them are presented. It is worth noting that because of repeated measurement, most of the possible errors can be covered and as it is mentioned before, in practice, identifying the position and severity of the impacts provides sufficient information for maintenance personnel and track inspection optimization schedule, which is the scope of the presented algorithm.

Finally, with the help of the presented index, the deterioration rate of each weld can be monitored in repeated data gathering and the inspection program and maintenance actions can be planned and optimized based on the intensity and rate of the index. This procedure can be applied and developed to any kind of rail surface defect and track. However, generalizing the values used for all kinds of tracks and fleet needs to be studied in more detail.

5. Conclusions

In this paper, with the help of field tests and the axle box acceleration method, impacts from rail welds are analyzed. At first, with the help of sensor fusion (vertical axle box accelerations and train position data), an odometry algorithm was developed. The proposed algorithm was based on detecting welds on the measured acceleration signal and maintained its performance for both straight and curved tracks. The use of the presented algorithm is essential in the implementation of the track condition monitoring system and rail defects monitoring. These accelerations are also used to identify rail weld defects. Using a nonlinear neural network-based regression model, it is found that acceleration amplitude has a linear relationship with velocity and the velocity-weighted accelerations due to weld impacts follow the Burr distribution. The 95% upper bound is selected as a criterion for faulty welds. In the next step, the wheel mode shape amplitude summation (WMAS) and velocity-weighted WMAS is calculated using FFT and results are compared. Based on the results, an index is defined for the health evaluation of rail welds. A limit speed is also defined to prevent large values at a very low speed. The results show that even welds at low train speeds can be compared with the ones at higher speeds. A comparison between the two methods is made, and results from comparing the welds, locally and generally, are discussed. The assumption of comparing welds in a local or the whole corridor can be applied to both presented criteria. Also, the upper bound limit for inspection can be adjusted depending on the reliability of welds or network, safety, workforce, and workload available. The presented methods are simple and practical and they can be applied to prioritize inspection schedules. Finally, an example is presented with another measurement data to practically present this method's advantages.

Data Availability

Due to privacy and ethical concerns, neither the data nor the source of the data can be made available.

Conflicts of Interest

The authors declare that there are no conflicts of interest regarding the publication of this paper.

References

[1] C. E. N. En, *13848-5, Railway Applications–Track–Track Geometry Quality–Part 5: Geometric Quality Levels–plain Line, Switches and Crossings*, Brussels European Commission Standard, Belgium, Europe, 2017.

[2] M. Molodova, Z. Li, A. Núñez, and R. Dollevoet, "Validation of a finite element model for axle box acceleration at squats in the high frequency range," *Computers & Structures*, vol. 141, pp. 84–93, 2014.

[3] M. Molodova, Z. Li, A. Núñez, and R. Dollevoet, "Parametric study of axle box acceleration at squats," *Proceedings of the Institution of Mechanical Engineers - Part F: Journal of Rail and Rapid Transit*, vol. 229, no. 8, pp. 841–851, 2015.

[4] M. Molodova, Z. Li, A. Núñez, and R. Dollevoet, "Automatic detection of squats in railway infrastructure," *IEEE Transactions on Intelligent Transportation Systems*, vol. 15, no. 5, pp. 1980–1990, 2014.

[5] M. Molodova, M. Oregui, A. Núñez, Z. Li, J. Moraal, and R. Dollevoet, "Axle box acceleration for health monitoring of insulated joints: a case study in The Netherlands," in *Proceedings of the 17th International IEEE Conference on Intelligent Transportation Systems (ITSC)*, pp. 822–827, Qingdao, China, October 2014.

[6] M. Molodova, Z. Li, A. Núñez, and R. Dollevoet, "Monitoring the railway infrastructure: detection of surface defects using wavelets," in *Proceedings of the 16th International IEEE Conference on Intelligent Transportation Systems (ITSC 2013)*, pp. 1316–1321, The Hague, Netherlands, June 2013.

[7] M. Oregui, S. Li, A. Núñez, Z. Li, R. Carroll, and R. Dollevoet, "Monitoring bolt tightness of rail joints using axle box acceleration measurements," *Structural Control and Health Monitoring*, vol. 24, no. 2, p. e1848, 2017.

[8] A. Nunez, T. Popa, L. E. Anghel et al., "Smart technology solutions for the NeTIRail-INFRA case study lines: axle box acceleration and ultra-low cost smartphones," *In Transport Research Arena 2018: A Digital Era for Transport*.

[9] P. Bocz, Á. Vinkó, and Z. Posgay, "A practical approach to tramway track condition monitoring: vertical track defects detection and identification using time-frequency processing technique," *Selected Scientific Papers - Journal of Civil Engineering*, vol. 13, no. s1, pp. 135–146, 2018.

[10] H. Cho and J. Park, "Study of rail squat characteristics through analysis of train axle box acceleration frequency," *Applied Sciences*, vol. 11, no. 15, p. 7022, 2021.

[11] X. Xu, J. Liu, S. Sun, L. Niu, and X. Mao, "Dynamic diagnosis method and quantitative characterization of rail corrugation," *Proceedings of the Institution of Mechanical Engineers - Part F: Journal of Rail and Rapid Transit*, vol. 0, no. 0, Article ID 095440972211079, 2022.

[12] C. Esveld and M. Steenbergen, "Force-based assessment of rail welds," in *Proceedings of 7th World Congress on Railway Research*, pp. 4–8, Montreal, Canada, June 2006.

[13] J. Otegui, A. Bahillo, I. Lopetegi, and L. E. Diez, "A survey of train positioning solutions," *IEEE Sensors Journal*, vol. 17, no. 20, pp. 6788–6797, 2017.

[14] A. Mirabadi, N. Mort, and F. Schmid, "Application of sensor fusion to railway systems," in *Proceedings of the 1996 IEEE/SICE/RSJ International Conference on Multisensor Fusion and Integration for Intelligent Systems (Cat. No. 96TH8242)*, pp. 185–192, Washington, DC, USA, August 1996.

[15] B. Allotta, V. Colla, and M. Malvezzi, "Train position and speed estimation using wheel velocity measurements," *Proceedings of the Institution of Mechanical Engineers - Part F: Journal of Rail and Rapid Transit*, vol. 216, no. 3, pp. 207–225, 2002.

[16] M. Malvezzi, B. Allotta, and M. Rinchi, "Odometric estimation for automatic train protection and control systems," *Vehicle System Dynamics*, vol. 49, no. 5, pp. 723–739, 2011.

[17] M. Malvezzi, G. Vettori, B. Allotta, L. Pugi, A. Ridolfi, and A. Rindi, "A localization algorithm for railway vehicles based on sensor fusion between tachometers and inertial measurement units," *Proceedings of the Institution of Mechanical Engineers - Part F: Journal of Rail and Rapid Transit*, vol. 228, no. 4, pp. 431–448, 2014.

[18] M. Shadfar and H. Molatefi, "Detection of rail local defects using in-service trains," *Proceedings of the Institution of Mechanical Engineers - Part F: Journal of Rail and Rapid Transit*, vol. 236, no. 9, pp. 1114–1123, 2022.

[19] M. Scholz, "Validation of nonlinear PCA," *Neural Processing Letters*, vol. 36, no. 1, pp. 21–30, 2012.

[20] P. Salvador, V. Naranjo, R. Insa, and P. Teixeira, "Axlebox accelerations: their acquisition and time–frequency characterisation for railway track monitoring purposes," *Measurement*, vol. 82, pp. 301–312, 2016.

[21] A. N. Morad Shadfar and H. Molatefi, "Effects of wheelset structural vibration on axle-box acceleration measurement," *Journal of Physics: Conf. Series*, vol. 1213, 2019.

[22] M. S. Habibollah Molatefi and R. Rostami, *The Effects of Rail weld Impacts on Wheel Structural Vibration*, in *Proceedings of the International Conference on Recent Advances in Railway Engineering*, Palma, Mallorca, Spain, September 2021.